Supporting Information

Boosting the Catalytic Performance of Ru Nanoparticles on the Cleavage of β-O-4 Linkage in Lignin by Doping Mo

Puyi Lei, Jiali Zhang, Wenzhuo Shen, Min Zhong, and Shouwu Guo*

Department of Electronic Engineering, School of Electronic Information and Electrical Engineering, Shanghai Jiao Tong University, Shanghai 200240, P. R. China.

*Correspondences should be addressed to: swguo@sjtu.edu.cn

Chemical reagents

Graphene oxide (GO) was prepared following the procedure described in our previous work[1]. Birch organosolv lignin extracted from commercially available pet birch sawdust following also a procedure we previous reported[2]. Briefly, 20 g crushed birch sawdust wrapped within filter paper was put into a Soxhlet extractor, and a mixture of 15 mL 2M HCl and 150 mL 1,4-dioxane was used as solvent. The solvent was heated to reflux under an atmosphere of N_2 for 1h. The mixture was then cooled and filtrated to acquire the slimy liquor. The collected liquor was then rotary evaporated to get a concentrated sticky residue. The residue was firstly dissolved into a mixture of 225 mL acetone and 25 mL water, and then 250 mL water was added with rapid stirring. The crude lignin was precipitated gradually, and was collected by vacuum filtration. Finally, the crude lignin was dissolved into a mixture of 9 mL acetone and 1 mL methanol, and the mixture was dropwise added into a flask with 200 mL diethyl ether under vigorously stirring. The pure lignin was precipitated, filtrated, dried under vacuum to obtain organosolv lignin (1.93 g, 9.7% yield).

Table S1

Table S1 Chemical reagents used in the work

Reagent	Purity	Producer
$NaBH_4$	99%	Sinopharm Chemical Reagent Co. Ltd.
CH_3CN	HPLC	
methanol	HPLC	
ethanol	95% & anhydrous	
benzoic acid	AR	
phenol	AR	
acetic acid	AR	
tert-butanol	CP	
2,2,6,6-tetramethylpiperidine (TEMP)	98%	Bide Pharmatech Co. Ltd.
$RuCl_3 \cdot 3H_2O$	99.99%	
5,5-dimethyl-1-pyrroline N-oxide(DMPO)	97%	
4-methoxylphenol	99%	
2-phenoxy-1-phenylethanol	97%	
$MoCl_5$	99.5%	Meryer Chemical Technology Co. Ltd.
sodium citrate	98%	Aladdin Bio-Chem

β-carotene	96%	Technology Co. Ltd.
iso-propanol	AR	
2-phenoxyacetophenone	98%	
benzoylformic acid	95%	
3,4-dimethoxybenzoic acid	99%	
3,5-dimethoxyphenol	98%	
3,4,5-trimethoxybenzoic acid	99%	
4-methoxybenzyl alcohol	97%	Shanghai Wokai Pharmaceutical Co. Ltd.
veratryl alcohol	98%	Sun Chemical Technology (Shanghai) Co. Ltd.
p-anisic acid	99%	Shanghai Macklin Biochemical Technology Co. Ltd.
silicon standard	99.9% metals basis	

Figure S1

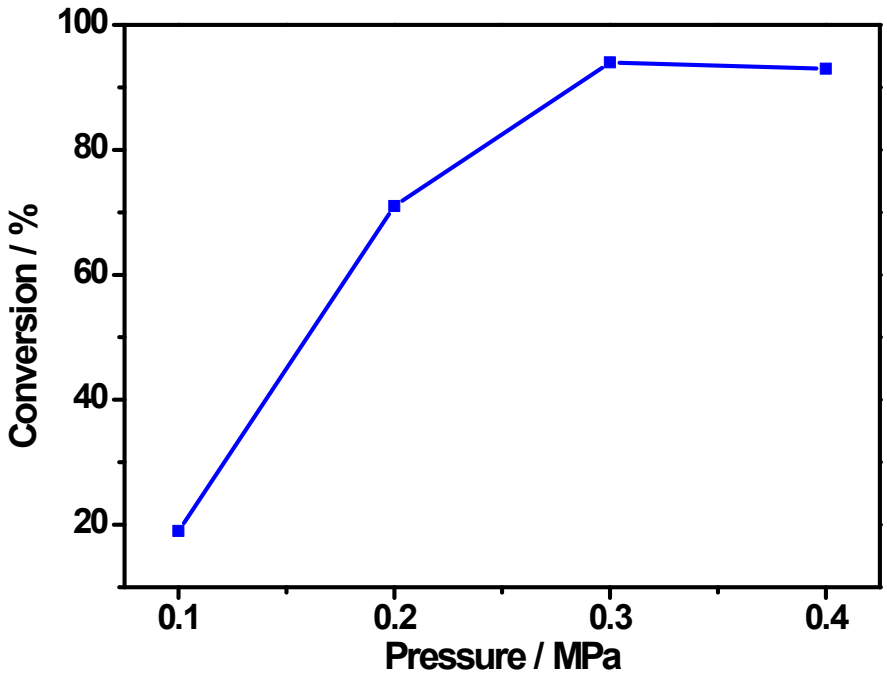

Figure S1 Effects of the O_2 Pressure on the oxidative oxidative cleavage of β-O-4 linkage. Condition: 0.2 mg RuMo/rGO (10-1), 0.1 mmol 2-phenoxy-1-phenylethanol, pH =12, 12h. Reactions were filled with different pressure oxygen previously.

Figure S2

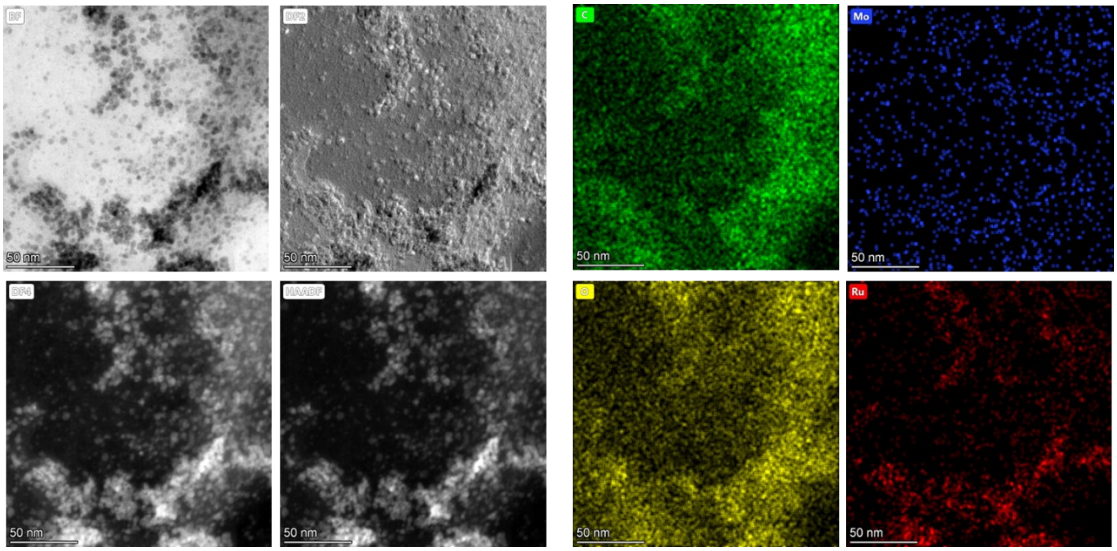

Figure S2 STEM images and element mappings of RuMo/rGO(10-1).

Figure S3

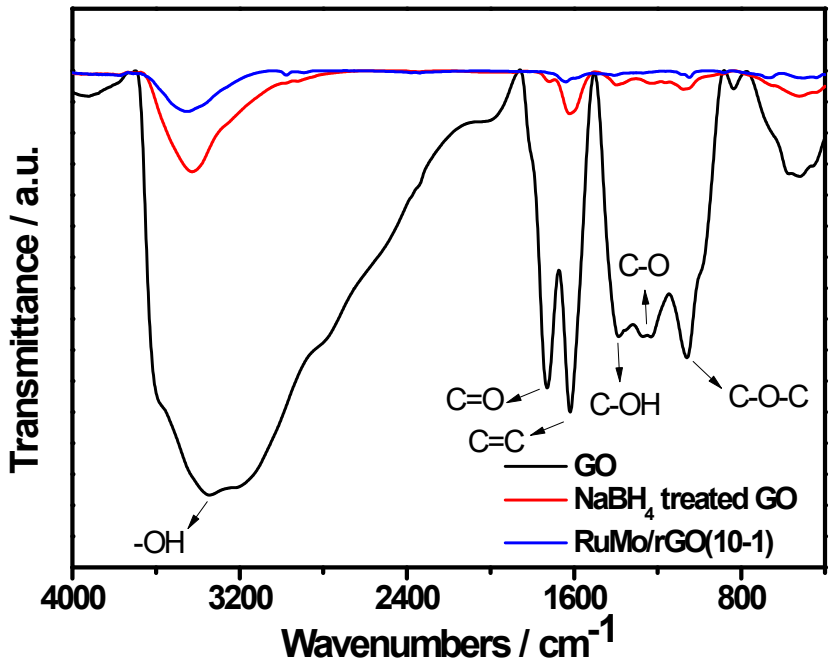

Figure S3 FTIR spectra of GO, reduced GO (rGO) with $NaBH_4$, and RuMo/rGO(10-1), respectively.

Table S2

Table S2 *g* factor value of EPR spectra

Entry	Catalyst	Trapping Agent	g^a
1	Mo-rGO	TEMP	2.0075
2	Ru-rGO	TEMP	2.0074
3	RuMo/rGO(10-1)	TEMP	2.0062
4	rGO	TEMP	2.0061
5	bare RuMo nanoparticles	TEMP	/[b]
6	rGO	DMPO	2.0064
7	RuMo/rGO(10-1)	DMPO	2.0063
8	bare RuMo nanoparticles	DMPO	/[b]

[a]obtained by the midpoint of the *g* factor-intensity illustrated in Figure S5. [b]No signal observed.

Figure S4

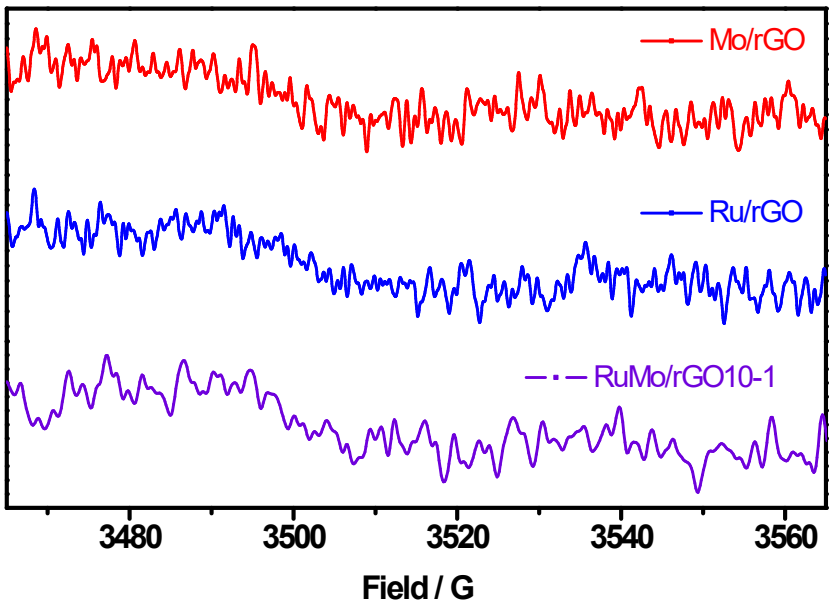

Figure S4 EPR spectra of DMPO (5%) in the presences of Mo/rGO, Ru/rGO, and RUMo/rGO(10-1) composites. Condition: 0.2 mg composite, 0.3 MPa O_2, 100℃, 0.5h, pH=12, 3 mL deionized water as solvent.

Figure S5

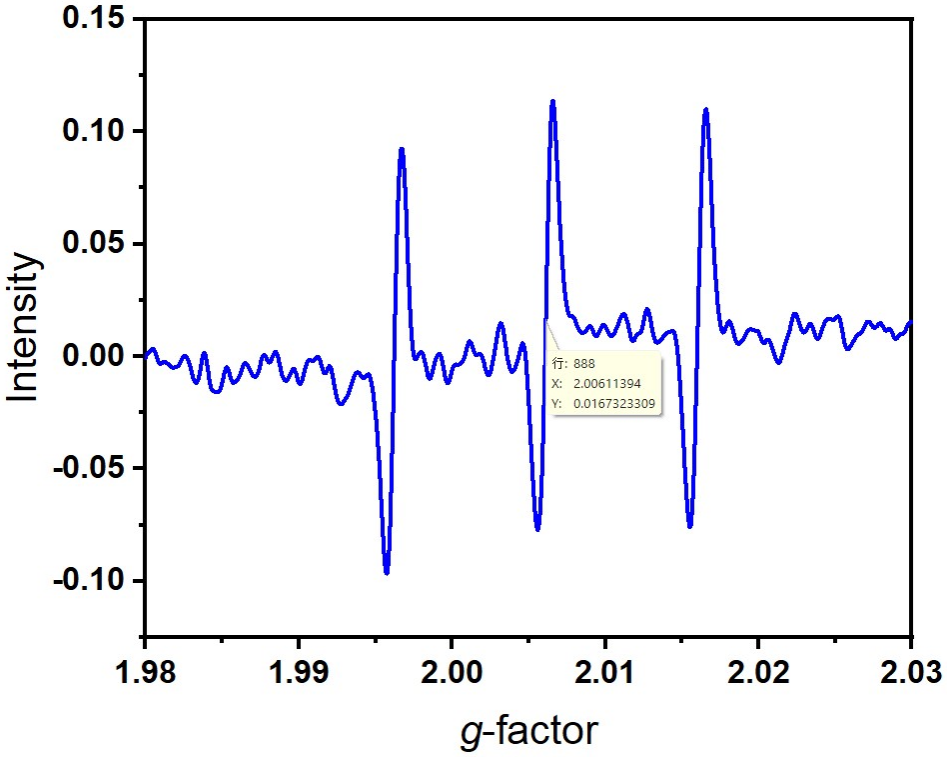

Figure S5 Diagrammatic illustration for *g* factor acquirements (Table S2, entry 4).

Figure S6

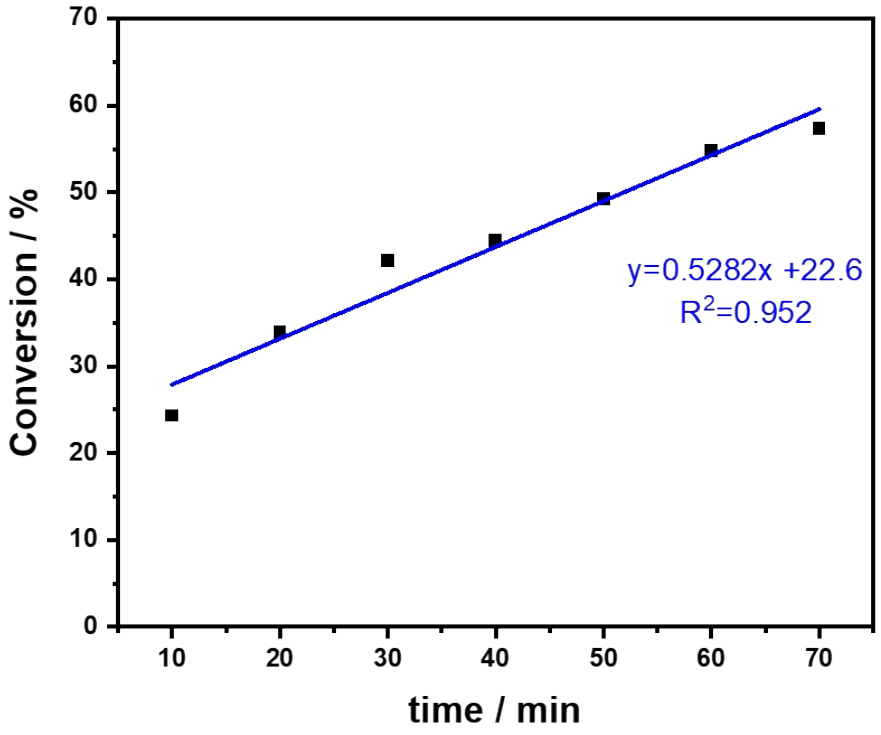

Figure S6 Operando-monitoring results of the oxidation reaction of 2-phenoxy-1-phenylethanol. Reaction conditions: 0.025 mmol 2-phenoxy-1-phenylethanol, 0.5 mg RuMo/rGO(10-1)(26.9% Ru, 4.3% Mo, calculated from ICP results), 5 mL deionized water, 0.3 MPa O_2, pH=12, 100℃, 12h. Reaction was operando-monitored by HPLC.

. **Table S3**

Table S3 Comparison on the reaction conditions for the oxidation cleavages of 2-phenoxy-1-phenylethanol using different catalysts

Entry	Catalyst	Base	Oxidant	Solvent	Temp. / ℃	Time / h	Conv. / %	TOF[h] / h^{-1}	Ref.
1	RuMo/rGO(10-1)[a]	NaOH	0.3 MPa O_2	H_2O	100	12	99	5.5	This work
2	Co/NG@3dNG-900[b]	-	0.3 MPa O_2	Methanol	120	4	100	1.0	[2]
3	Au/CeO_2[c]	-	1 MPa O_2	Methanol	180	4	71.5	14.8	[3]
4	Au-Pd-CTF[d]	-	0.5 MPa O_2	Methanol	160	4	96	19.4[i]	[4]
5	Pd/CeO_2[e]	-	0.1 MPa O_2	Methanol	185	24	64	0.6	[5]
6	Co-N-C[f]	NaOH	1 MPa Air	Methanol	150	4	93	4.4	[6]
7	WO_3[g]	NaOH	TBHP	H_2O	80	3	97	1.6	[7]

Reaction conditions: [a]0.025 mmol 2-phenoxy-1-phenylethanol, 0.5 mg RuMo/rGO(10-1)(26.9% Ru, 4.3% Mo, calculated from ICP results), 3 mL deionized water, 0.3 MPa O_2, pH=12, 100℃, 12h. [b]0.01 mmol 2-phenoxy-1-phenylethanol, 3 mg Co/NG@3dNG-900 (25.7 mol% of Co to 2-phenoxy-1-phenylethanol), 3 mL CH_3OH, 0.3 MPa O_2, 120 ℃, 4 h. [c]0.47 mmol 2-phenoxy-1-phenylethanol, 20 mg Au/CeO_2 (0.88 wt% of Au), 25 mL CH_3OH, 1 MPa O_2, 180 ℃, 4 h. [d]0.2 mmol 2-phenoxy-1-phenylethanol, 40 mg Au-Pd-CTF, 5 mL CH_3OH, 0.5 MPa O_2, 160 °C, 4 h. [e]0.6 mmol 2-phenoxy-1-phenylethanol, 0.2 g Pd/CeO_2 (1.5 wt% of Pd), 50 mL CH_3OH, 0.1 MPa O_2, 185 ℃, 24 h. [f]0.2 mmol 2-phenoxy-1-phenylethanol, 20 mg Co-N-C (3.1 wt%), 0.2 mmol NaOH, 5 mL CH_3OH, 1 MPa air, 150 °C, 4 h. [g]0.5 mmol 2-phenoxy-1-phenylethanol, 0.1 mmol nano WO_3, 3.9 mmol TBHP (70%), 4.8 mmol NaOH (24%), 80 °C, 3 h. [h]The turnover frequency (TOF) was estimated or calculated from data provided in the original articles. TOF of catalyst is calculated as the mmol of 2-phenoxy-1-phenylethanol consumed by 1 mmol of active metal/metal oxide in

the catalyst (active metal/metal oxide loading) per hour. [i]Given by original literature.

Figure S7

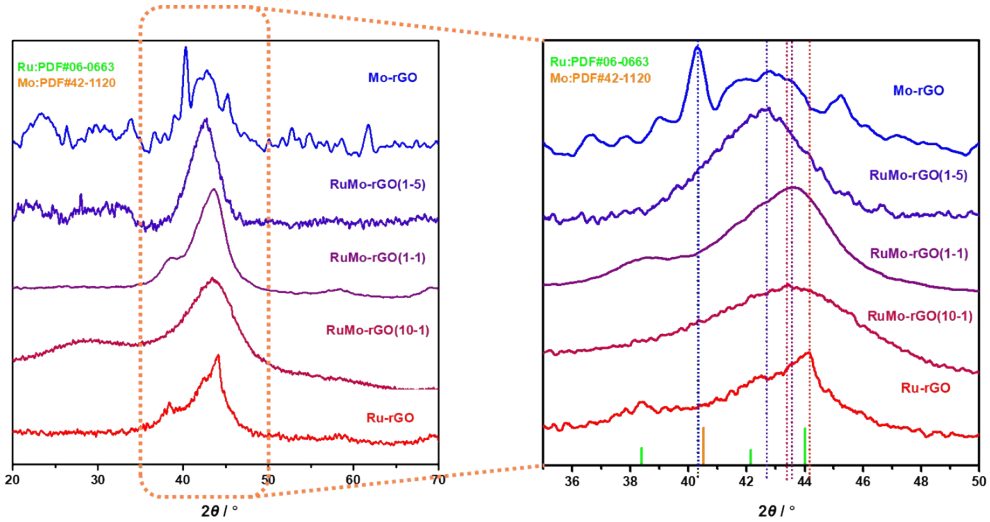

Figure S7 XRD patterns of RuMo/rGO composites with different Ru to Mo ratios. Figure S7b is enlarged paattern of Figure S7a at 2θ =35-50°. The patterns were normalized using silicon as internal standard (5% wt).

Figure S8

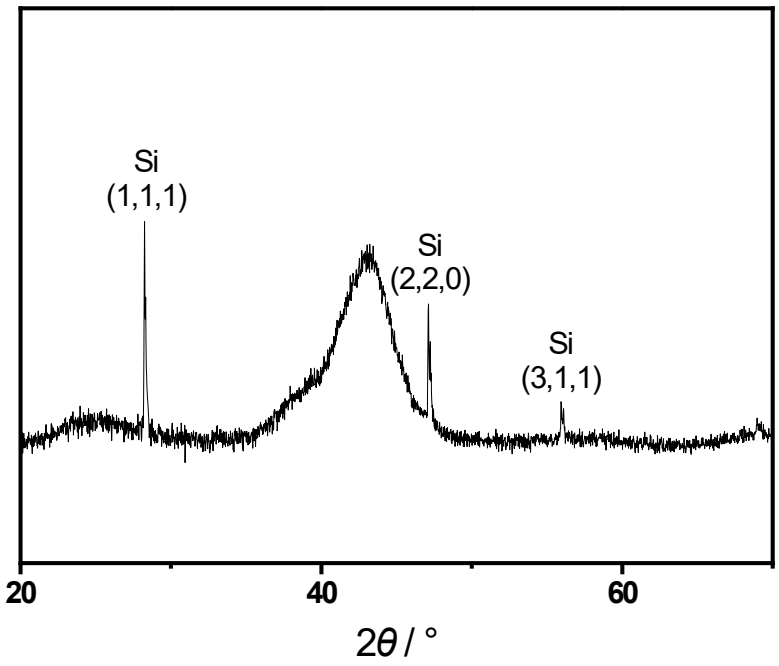

Figure S8 XRD patterns of RuMo/rGO(10-1) with 5% wt. of silicon as internal standard agent.

Table S4

Table S4. Detailed Ru and Mo contents in the RuMo/rGO composites determined with ICP-OES measurement and the feeding ratios of Ru and Mo during the fabrications

Entry	1	2	3	4	5	6	7
Sample	RuMo/rGO(10-1)	RuMo/rGO(5-1)	RuMo/rGO(3-1)	RuMo/rGO(1-1)	RuMo/rGO(1-3)	RuMo/rGO(1-5)	RuMo/rGO(1-10)
Feed Ratio (Ru: Mo)	10:1	5:1	3:1	1:1	1:3	1:5	1:10
ICP Ratio (Ru: Mo)	6.25:1	5.66:1	4.03:1	1.31:1	1:1.20	1:2.98	1:15.48

Figure S9

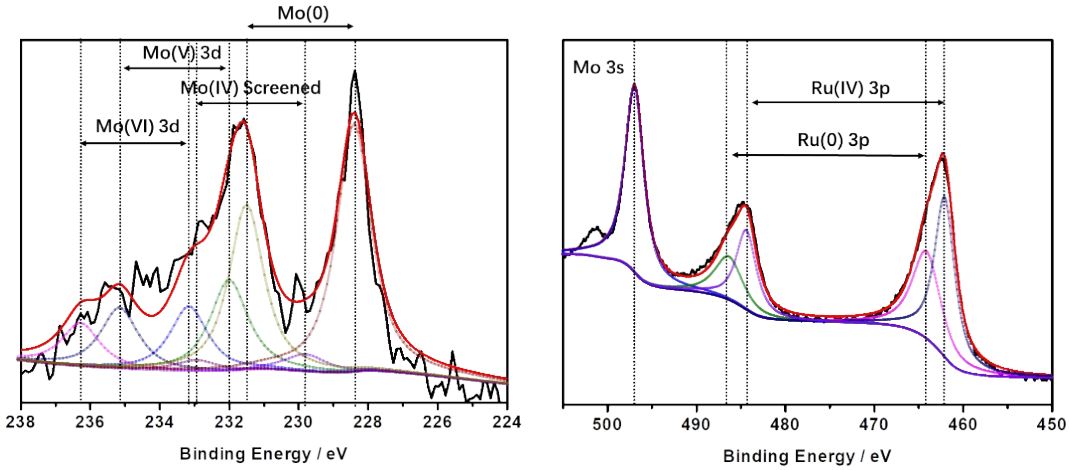

Figure S9 XPS spectra of Mo 3*d* and Ru 3*p* of RuMo/rGO(10-1).

Table S5

Table S5 XPS data of RuMo/rGO(10-1).

	Peak	Binding energy / eV	FWHM / eV	Distribution
Mo(VI)	3*d* 5/2	236.3	1.29	16%
	3*d* 3/2	233.2	1.29	
Mo(V)	3*d* 5/2	235.2	1.29	23%
	3*d* 3/2	232.0	1.29	
Mo(IV)	3*d* 5/2	232.9	1.49	5%
Screened	3*d* 3/2	229.8	1.49	
Mo(0)	3*d* 5/2	231.5	1.19	56%
	3*d* 3/2	228.4	1.19	
Ru(IV)	3*p* 1/2	484.3	2.73	43%
	3*p* 3/2	462.1	2.73	
Ru(0)	3*p* 1/2	486.3	3.78	57%
	3*p* 3/2	464.1	3.78	
Mo	3*s*	497.0	2.49	/

Table S6

Table S6 Retention time (t_R) and mobile phase information of HPLC measurement

Reagent	t_R[a] / min	Mobile phase (A: 0.5% aqueous acetic acid; B: acetonitrile)[b] / %	
		A	B
2-phenoxy-1-phenylethanol **(1)**	14.2	60	40
2	13.8	60	40
3	14.5	60	40
4	13.5	60	40
5	15.5	60	40
6	11.3	60	40
7	13.0	60	40
2-phenoxy-1-phenylethan-1-one	18.6	60	40
α-hydroxyacetophenone	2.9	60	40
benzoic acid	7.7	60	40
phenol	6.3	60	40
p-benzoquinone	3.67	60	40
guaiacol	6.0	60	40
4-methoxyphenol	7.7	60	40

3,5-dimethoxyphenol	6.3	60	40
veratric acid	5.0	60	40
3,4,5-trimethoxybenzoic acid	7.8	60	40

[a]t_R±0.1 min. The data were acquired at λ = 273 nm, and calibrated using internal standard method. [b]Solvent was previously mixed and pre-heated to 25℃ to avoid endothermal disturbance during mixing acetonitrile and water.

Figure S10

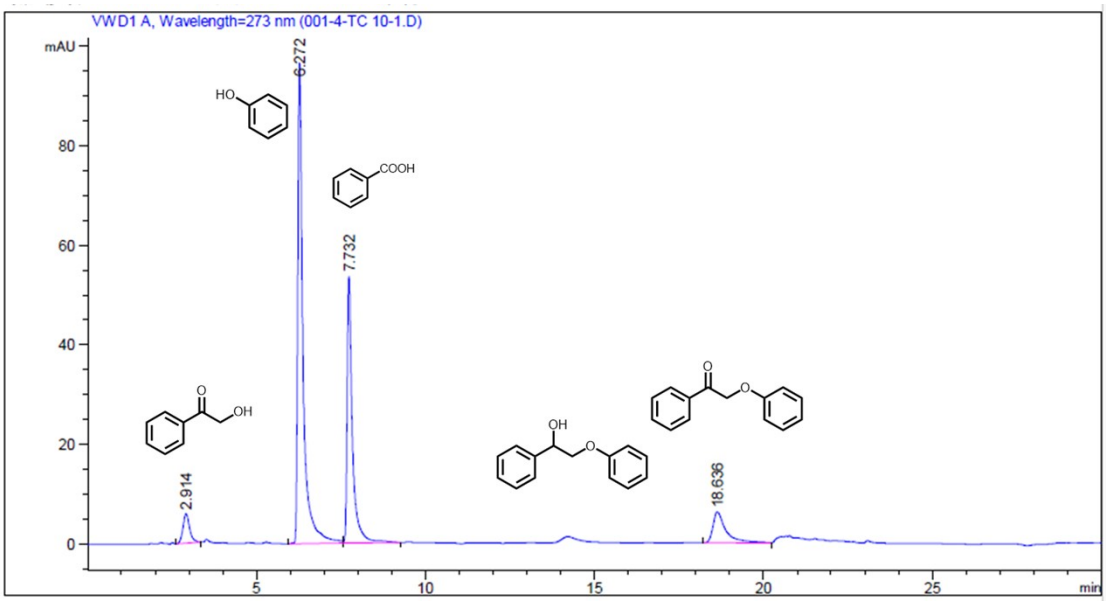

Figure S10 HPLC spectrum of 2-phenoxy-1-phenylethanol oxidation reaction catalyzed by RuMo/rGO(10-1). Reaction conditions: 0.2 mg RuMo/rGO(10-1), 0.01mmol 2-phenoxy-1-phenylethanol, 0.3 MPa O_2, 100℃, 12h, pH =12, detection wavelength = 273 nm, using CH_3CN: 0.5% CH_3COOH = 40:60, v/v as mobile phase. The reaction solution was previously neutralized by 0.1M HCl, filtrated, attenuated to corresponding mobile phase solvent ratio (CH_3CN:0.5% CH_3COOH = 40:60, v/v) with CH_3CN, and then used for HPLC. Products were identified using internal standard method with corresponding reagents as internal standard substances.

Figure S11

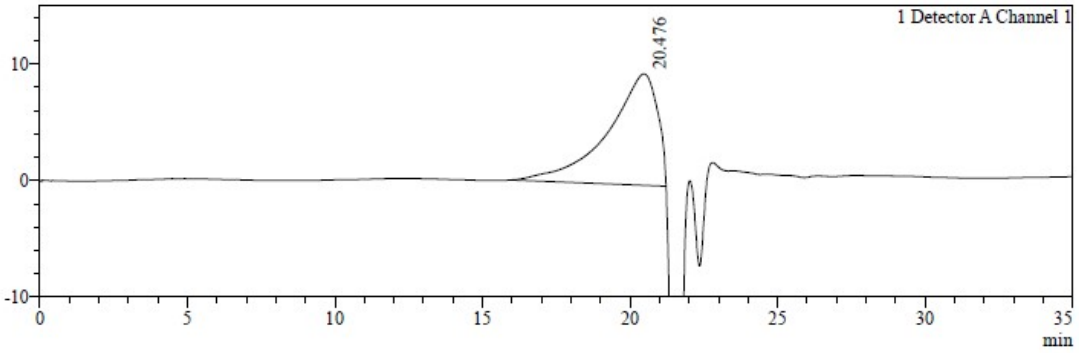

Figure S11 GPC data of as-extracted organosolv lignin using DMF as eluent.

Figure S12

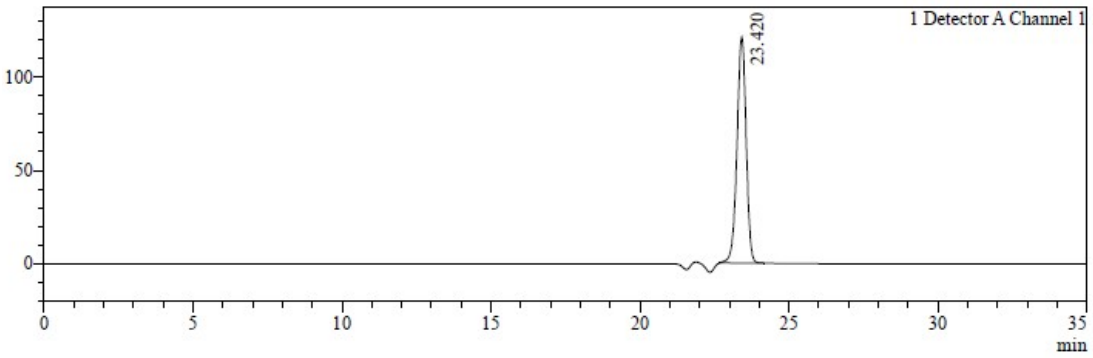

Figure S12 GPC data of organosolv lignin after the oxidation depolymerization with the RuMo/rGO(10-1) as catalyst and using DMF as eluent. Reaction conditions: 10 mg as-extracted organosolv lignin, 1 mg RuMo/rGO(10-1), 3 mL water, 0.3 MPa O_2, 100°C, 12 h, pH = 12.

Computational Details： Vienna Ab initio Simulation Package (VASP)[8-11] was utilized to perform DFT within periodic models in this work. Generalized gradient approximation (GGA)[12] with projector augmented wave (PAW)[13, 14] method was applied in calculations to better simulate the electronic statues and the core-electron interaction of the catalysts. The cutoff energy was set to be 450 eV. Spin polarization effect was considered in this work. The lattice parameters of graphite were optimized, and the results are consistent with experiments. The optimized cells were used to construct single-layer 6×6 graphene model and the structures with Ru and RuMo alloy clusters on the graphene. Herein, the metal cluster consisting of totally 30 metal atoms, for pure Ru cluster containing 30 Ru atoms, for RuMo is composed of 27 Ru atoms and 3 Mo atoms to simulate the RuMo/rGO(10-1). The Ru (0,0,1) lattice was used during the simulation in consideration of high ratio between Ru and Mo. Structural optimizations were performed until the residual forces on each ion converged to smaller than 0.05 eV $Å^{-1}$. Gamma k-points was used to describe the surface Brillouin zone. The width of vacuum layer was set larger than 12 Å to avoid spurious interaction.

The adsorption energies of intermediate species on the considered slabs are defined as:

$$E_{ads} = E_{slab+molec} - E_{slab} - E_{molec(g)}$$

where $E_{slab+molec}$ means the total energy of slab and adsorbed species, E_{slab} denotes the slab energy, and $E_{molec(g)}$ represents the energy of the species in gas phase.

2-Phenoxy-1-phenylethanol adsorbing on the surfaces of RuMo(9:1) and pure Ru

were optimized and simulated with similar methods. Results were summarized in Table S7. Atom coordinates of measured models were described in Table S8-S11.

Figure S13

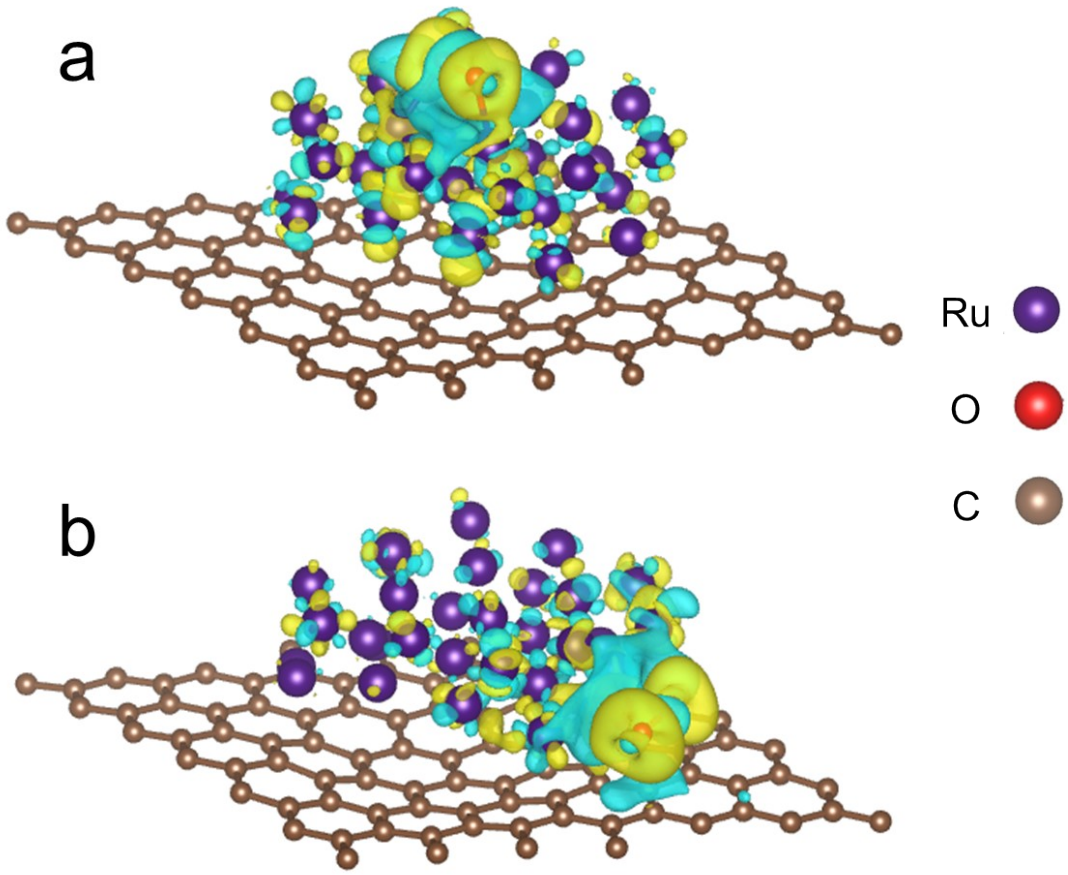

Figure S13 Different charge distributions of molecular oxygen adsorbing on (a) top of the Ru nanoparticle, and (b) at interface of Ru nanoparticles and rGO calculated by DFT. The model RuMo alloy nanoparticle is consisted of 30 Ru atoms to simulate the structure of Ru/rGO. Electron accumulation and depletion are represented in yellow and cyan, respectively.

Table S7

Table S7 Adsorption energy of 2-phenoxy-1-phenylethanol on RuMo and pure Ru surface.

Surface	Pure Ru	RuMo (9:1)
E_{ads} / eV	-2.89	-3.43

Table S8

Table S8 Coordinates for the optimized structure of Ru:Mo(9:1)-top model

Atom	*x*	*y*	*z*	Atom	*x*	*y*	*z*
C1	0.38633	0.09796	0.06729	C53	0.49733	0.65502	0.04848
C2	0.6647	0.15331	0.0712	C54	0.55369	0.7654	0.05446
C3	0.49764	0.98829	0.07255	C55	0.22075	0.26443	0.0664
C4	0.55336	0.09834	0.06982	C56	0.66502	0.65472	0.04494
C5	0.66553	0.98724	0.07188	C57	0.72068	0.76575	0.05103
C6	0.72046	0.09861	0.07338	C58	0.83029	0.6544	0.0631
C7	0.83139	0.98714	0.0651	C59	0.38703	0.93326	0.07416
C8	0.88657	0.09779	0.07155	C60	0.88663	0.76532	0.06274
C9	0.72055	0.26429	0.07007	C61	0.33064	0.1539	0.06434
C10	0.22026	0.09823	0.06685	C62	0.05321	0.93134	0.0686
C11	0.83129	0.15331	0.07429	C63	0.83164	0.82117	0.05726
C12	0.8866	0.26409	0.07697	C64	0.99703	0.65462	0.08207
C13	0.99747	0.15312	0.07295	C65	0.0527	0.76552	0.07763
C14	0.05285	0.26398	0.07678	C66	0.16373	0.82089	0.07849
C15	0.165	0.31993	0.07378	C67	0.49933	0.82041	0.06848
C16	0.22145	0.43181	0.07087	C68	0.55393	0.9321	0.07318
C17	0.33034	0.32042	0.05777	C69	0.88704	0.93188	0.06224
C18	0.38613	0.432	0.05192	C70	0.99748	0.82071	0.06988
C19	0.4978	0.32191	0.05739	C71	0.16433	0.9869	0.07002
C20	0.55408	0.4333	0.04698	C72	0.33094	0.98778	0.07175
C21	0.66551	0.32041	0.06261	Mo1	0.24475	0.40501	0.29316

C22	0.21949	0.93171	0.07326	Mo2	0.46282	0.81678	0.2628
C23	0.72001	0.43263	0.05967	Mo3	0.66567	0.60142	0.28659
C24	0.83164	0.31989	0.07508	O1	0.51271	0.53751	0.37552
C25	0.88692	0.43135	0.07764	O2	0.62213	0.57452	0.37155
C26	0.99785	0.98721	0.06645	Ru1	0.34407	0.48383	0.20266
C27	0.99711	0.31935	0.07925	Ru2	0.35436	0.30782	0.30616
C28	0.66481	0.82087	0.05486	Ru3	0.43522	0.3858	0.20935
C29	0.05243	0.4308	0.08224	Ru4	0.52761	0.30399	0.15385
C30	0.16428	0.48596	0.07939	Ru5	0.72907	0.39204	0.14779
C31	0.22092	0.59826	0.08223	Ru6	0.35466	0.78996	0.17003
C32	0.33196	0.48764	0.05801	Ru7	0.35113	0.61779	0.27952
C33	0.38636	0.59872	0.05667	Ru8	0.4572	0.69717	0.18952
C34	0.38564	0.26492	0.05894	Ru9	0.55339	0.59061	0.20027
C35	0.49751	0.48793	0.04471	Ru10	0.55614	0.38843	0.29069
C36	0.55324	0.59924	0.04304	Ru11	0.64382	0.47579	0.19903
C37	0.0534	0.09799	0.06949	Ru12	0.75881	0.49359	0.27962
C38	0.6647	0.48869	0.04825	Ru13	0.84142	0.58443	0.18151
C39	0.49705	0.15292	0.06702	Ru14	0.43693	0.22562	0.2379
C40	0.72063	0.59912	0.04924	Ru15	0.56616	0.89103	0.16755
C41	0.83032	0.48684	0.07293	Ru16	0.55902	0.71443	0.27984
C42	0.88508	0.5993	0.07719	Ru17	0.65617	0.78959	0.18917
C43	0.99747	0.48707	0.08283	Ru18	0.75051	0.68236	0.19408
C44	0.05291	0.59861	0.08425	Ru19	0.75686	0.79504	0.27988
C45	0.16373	0.65406	0.08425	Ru20	0.16404	0.40001	0.16245

C46	0.33137	0.82165	0.07852	Ru21	0.86165	0.68507	0.27387
C47	0.16481	0.15381	0.06784	Ru22	0.25861	0.71586	0.26165
C48	0.21912	0.76526	0.08208	Ru23	0.45025	0.49879	0.29436
C49	0.3314	0.6527	0.07029	Ru24	0.6602	0.91212	0.26425
C50	0.72075	0.93166	0.06415	Ru25	0.23461	0.2916	0.21835
C51	0.38699	0.76459	0.07388	Ru26	0.14811	0.47882	0.26599
C52	0.55272	0.26469	0.06321	Ru27	0.25632	0.59587	0.18319

Table S9 Coordinates for the optimized structure of Ru:Mo(9:1)-interface model

Atom	***x***	***y***	***z***	**Atom**	***x***	***y***	***z***
C1	0.38633	0.09796	0.06729	C53	0.49733	0.65502	0.04848
C2	0.6647	0.15331	0.0712	C54	0.55369	0.7654	0.05446
C3	0.49764	0.98829	0.07255	C55	0.22075	0.26443	0.0664
C4	0.55336	0.09834	0.06982	C56	0.66502	0.65472	0.04494
C5	0.66553	0.98724	0.07188	C57	0.72068	0.76575	0.05103
C6	0.72046	0.09861	0.07338	C58	0.83029	0.6544	0.0631
C7	0.83139	0.98714	0.0651	C59	0.38703	0.93326	0.07416
C8	0.88657	0.09779	0.07155	C60	0.88663	0.76532	0.06274
C9	0.72055	0.26429	0.07007	C61	0.33064	0.1539	0.06434
C10	0.22026	0.09823	0.06685	C62	0.05321	0.93134	0.0686
C11	0.83129	0.15331	0.07429	C63	0.83164	0.82117	0.05726
C12	0.8866	0.26409	0.07697	C64	0.99703	0.65462	0.08207
C13	0.99747	0.15312	0.07295	C65	0.0527	0.76552	0.07763
C14	0.05285	0.26398	0.07678	C66	0.16373	0.82089	0.07849

C15	0.165	0.31993	0.07378	C67	0.49933	0.82041	0.06848
C16	0.22145	0.43181	0.07087	C68	0.55393	0.9321	0.07318
C17	0.33034	0.32042	0.05777	C69	0.88704	0.93188	0.06224
C18	0.38613	0.432	0.05192	C70	0.99748	0.82071	0.06988
C19	0.4978	0.32191	0.05739	C71	0.16433	0.9869	0.07002
C20	0.55408	0.4333	0.04698	C72	0.33094	0.98778	0.07175
C21	0.66551	0.32041	0.06261	Mo1	0.24475	0.40501	0.29316
C22	0.21949	0.93171	0.07326	Mo2	0.46282	0.81678	0.2628
C23	0.72001	0.43263	0.05967	Mo3	0.66567	0.60142	0.28659
C24	0.83164	0.31989	0.07508	O1	0.4541	0.94893	0.25905
C25	0.88692	0.43135	0.07764	O2	0.45463	0.95747	0.19528
C26	0.99785	0.98721	0.06645	Ru1	0.34407	0.48383	0.20266
C27	0.99711	0.31935	0.07925	Ru2	0.35436	0.30782	0.30616
C28	0.66481	0.82087	0.05486	Ru3	0.43522	0.3858	0.20935
C29	0.05243	0.4308	0.08224	Ru4	0.52761	0.30399	0.15385
C30	0.16428	0.48596	0.07939	Ru5	0.72907	0.39204	0.14779
C31	0.22092	0.59826	0.08223	Ru6	0.35466	0.78996	0.17003
C32	0.33196	0.48764	0.05801	Ru7	0.35113	0.61779	0.27952
C33	0.38636	0.59872	0.05667	Ru8	0.4572	0.69717	0.18952
C34	0.38564	0.26492	0.05894	Ru9	0.55339	0.59061	0.20027
C35	0.49751	0.48793	0.04471	Ru10	0.55614	0.38843	0.29069
C36	0.55324	0.59924	0.04304	Ru11	0.64382	0.47579	0.19903
C37	0.0534	0.09799	0.06949	Ru12	0.75881	0.49359	0.27962
C38	0.6647	0.48869	0.04825	Ru13	0.84142	0.58443	0.18151

C39	0.49705	0.15292	0.06702	Ru14	0.43693	0.22562	0.2379
C40	0.72063	0.59912	0.04924	Ru15	0.56616	0.89103	0.16755
C41	0.83032	0.48684	0.07293	Ru16	0.55902	0.71443	0.27984
C42	0.88508	0.5993	0.07719	Ru17	0.65617	0.78959	0.18917
C43	0.99747	0.48707	0.08283	Ru18	0.75051	0.68236	0.19408
C44	0.05291	0.59861	0.08425	Ru19	0.75686	0.79504	0.27988
C45	0.16373	0.65406	0.08425	Ru20	0.16404	0.40001	0.16245
C46	0.33137	0.82165	0.07852	Ru21	0.86165	0.68507	0.27387
C47	0.16481	0.15381	0.06784	Ru22	0.25861	0.71586	0.26165
C48	0.21912	0.76526	0.08208	Ru23	0.45025	0.49879	0.29436
C49	0.3314	0.6527	0.07029	Ru24	0.6602	0.91212	0.26425
C50	0.72075	0.93166	0.06415	Ru25	0.23461	0.2916	0.21835
C51	0.38699	0.76459	0.07388	Ru26	0.14811	0.47882	0.26599
C52	0.55272	0.26469	0.06321	Ru27	0.25632	0.59587	0.18319

Table S10

Table S10 Coordinates for the optimized structure of Pure Ru-top model

Atom	*x*	*y*	*z*	Atom	*x*	*y*	*z*
C1	0.71991	0.26409	0.07045	C53	0.71984	0.76552	0.05203
C2	0.21937	0.09799	0.06533	C54	0.66467	0.98677	0.07313
C3	0.83045	0.15301	0.07439	C55	0.82955	0.6543	0.06411
C4	0.88592	0.26391	0.07655	C56	0.38619	0.93316	0.07438
C5	0.9966	0.15284	0.07191	C57	0.88596	0.76534	0.0635
C6	0.052	0.26377	0.07534	C58	0.32985	0.15382	0.06369
C7	0.16381	0.31952	0.0716	C59	0.83094	0.82099	0.05789
C8	0.22039	0.43146	0.06996	C60	0.99628	0.65464	0.08315
C9	0.32971	0.32034	0.05684	C61	0.05195	0.76559	0.07839
C10	0.3854	0.43183	0.05137	C62	0.33001	0.98763	0.07144
C11	0.49713	0.32185	0.05888	C63	0.1629	0.82094	0.07879
C12	0.55325	0.43314	0.04829	C64	0.49832	0.82041	0.06791
C13	0.66469	0.3203	0.06379	C65	0.71976	0.09835	0.07409
C14	0.21861	0.93154	0.07263	C66	0.55315	0.93171	0.07354
C15	0.71915	0.43254	0.06067	C67	0.88632	0.93169	0.06246
C16	0.83095	0.31975	0.07503	C68	0.99677	0.82071	0.07016
C17	0.8863	0.4312	0.0777	C69	0.38545	0.09792	0.06723
C18	0.99714	0.98708	0.06581	C70	0.66405	0.15314	0.0717
C19	0.99627	0.31915	0.07821	C71	0.83055	0.98682	0.06572
C20	0.66404	0.82069	0.0558	C72	0.8858	0.09756	0.07156

C21	0.05164	0.43061	0.08123	O1	0.56416	0.57736	0.36107
C22	0.1632	0.4856	0.07824	O2	0.57093	0.68052	0.36405
C23	0.21984	0.59791	0.08112	Ru1	0.65992	0.90849	0.26444
C24	0.3311	0.48752	0.05728	Ru2	0.23412	0.29747	0.21703
C25	0.38541	0.59849	0.05618	Ru3	0.15202	0.48152	0.25902
C26	0.55193	0.2645	0.06429	Ru4	0.26025	0.59736	0.1793
C27	0.38498	0.26492	0.05897	Ru5	0.35072	0.48656	0.20187
C28	0.49674	0.48779	0.04522	Ru6	0.35592	0.3052	0.30789
C29	0.55238	0.59911	0.04362	Ru7	0.43424	0.38066	0.21048
C30	0.05255	0.09786	0.06812	Ru8	0.53135	0.30324	0.1563
C31	0.66371	0.48866	0.04956	Ru9	0.72967	0.39493	0.14874
C32	0.4969	0.98811	0.07306	Ru10	0.36004	0.79242	0.16908
C33	0.49636	0.15288	0.0678	Ru11	0.34703	0.61476	0.2784
C34	0.71974	0.59903	0.05033	Ru12	0.4592	0.69594	0.18948
C35	0.82977	0.48679	0.07331	Ru13	0.25737	0.41136	0.29475
C36	0.88455	0.59932	0.07759	Ru14	0.46207	0.81204	0.26446
C37	0.05252	0.9313	0.06793	Ru15	0.66446	0.60065	0.2867
C38	0.99679	0.48689	0.08251	Ru16	0.55338	0.59016	0.20102
C39	0.05215	0.59845	0.08456	Ru17	0.55409	0.39534	0.29389
C40	0.16268	0.6538	0.08425	Ru18	0.64654	0.4767	0.20195
C41	0.3303	0.82153	0.07854	Ru19	0.76808	0.50108	0.2795
C42	0.16382	0.15356	0.06601	Ru20	0.84474	0.58786	0.1813
C43	0.55264	0.0981	0.07049	Ru21	0.44094	0.22565	0.24159
C44	0.21829	0.76522	0.08256	Ru22	0.56286	0.88989	0.16938

C45	0.33033	0.65239	0.07005	Ru23	0.56409	0.71222	0.28004
C46	0.71999	0.93131	0.06516	Ru24	0.65626	0.78967	0.18778
C47	0.38606	0.76463	0.07397	Ru25	0.7505	0.6813	0.19325
C48	0.49648	0.65496	0.04855	Ru26	0.75942	0.79685	0.27641
C49	0.55272	0.76536	0.05465	Ru27	0.16695	0.39856	0.16284
C50	0.16354	0.9868	0.06882	Ru28	0.86165	0.68801	0.27419
C51	0.2197	0.26421	0.06443	Ru29	0.25587	0.70979	0.25833
C52	0.66408	0.65452	0.04593	Ru30	0.45489	0.49632	0.29408

Table S11

Table S11 Coordinates for the optimized structure of Pure Ru-interface model

Atom	*x*	*y*	*z*	Atom	*x*	*y*	*z*
C1	0.66469	0.3203	0.06379	C53	0.99628	0.65464	0.08315
C2	0.21861	0.93154	0.07263	C54	0.32971	0.32034	0.05684
C3	0.71915	0.43254	0.06067	C55	0.05195	0.76559	0.07839
C4	0.83095	0.31975	0.07503	C56	0.33001	0.98763	0.07144
C5	0.8863	0.4312	0.0777	C57	0.1629	0.82094	0.07879
C6	0.99714	0.98708	0.06581	C58	0.49832	0.82041	0.06791
C7	0.99627	0.31915	0.07821	C59	0.71976	0.09835	0.07409
C8	0.66404	0.82069	0.0558	C60	0.55315	0.93171	0.07354
C9	0.05164	0.43061	0.08123	C61	0.88632	0.93169	0.06246
C10	0.1632	0.4856	0.07824	C62	0.88592	0.26391	0.07655
C11	0.21984	0.59791	0.08112	C63	0.99677	0.82071	0.07016
C12	0.3311	0.48752	0.05728	C64	0.38545	0.09792	0.06723
C13	0.38541	0.59849	0.05618	C65	0.3854	0.43183	0.05137
C14	0.55193	0.2645	0.06429	C66	0.66405	0.15314	0.0717
C15	0.38498	0.26492	0.05897	C67	0.83055	0.98682	0.06572
C16	0.49674	0.48779	0.04522	C68	0.8858	0.09756	0.07156
C17	0.55238	0.59911	0.04362	C69	0.9966	0.15284	0.07191
C18	0.05255	0.09786	0.06812	C70	0.052	0.26377	0.07534
C19	0.66371	0.48866	0.04956	C71	0.49713	0.32185	0.05888
C20	0.4969	0.98811	0.07306	C72	0.55325	0.43314	0.04829

C21	0.49636	0.15288	0.0678	Mo1	0.43922	0.98319	0.18967
C22	0.71974	0.59903	0.05033	Mo2	0.33811	0.90415	0.20344
C23	0.82977	0.48679	0.07331	Mo3	0.6644	0.6014	0.2867
C24	0.88455	0.59932	0.07759	O1	0.55338	0.59016	0.20102
C25	0.05252	0.9313	0.06793	O2	0.55409	0.39534	0.29389
C26	0.71991	0.26409	0.07045	Ru1	0.64654	0.4767	0.20195
C27	0.99679	0.48689	0.08251	Ru2	0.76808	0.50108	0.2795
C28	0.05215	0.59845	0.08456	Ru3	0.84474	0.58786	0.1813
C29	0.16268	0.6538	0.08425	Ru4	0.44094	0.22565	0.24159
C30	0.3303	0.82153	0.07854	Ru5	0.56286	0.88989	0.16938
C31	0.16382	0.15356	0.06601	Ru6	0.56409	0.71222	0.28004
C32	0.16381	0.31952	0.0716	Ru7	0.65626	0.78967	0.18778
C33	0.55264	0.0981	0.07049	Ru8	0.7505	0.6813	0.19325
C34	0.21829	0.76522	0.08256	Ru9	0.75942	0.79685	0.27641
C35	0.33033	0.65239	0.07005	Ru10	0.16695	0.39856	0.16284
C36	0.71999	0.93131	0.06516	Ru11	0.86165	0.68801	0.27419
C37	0.38606	0.76463	0.07397	Ru12	0.25587	0.70979	0.25833
C38	0.21937	0.09799	0.06533	Ru13	0.45489	0.49632	0.29408
C39	0.49648	0.65496	0.04855	Ru14	0.65992	0.90849	0.26444
C40	0.55272	0.76536	0.05465	Ru15	0.23412	0.29747	0.21703
C41	0.16354	0.9868	0.06882	Ru16	0.15202	0.48152	0.25902
C42	0.2197	0.26421	0.06443	Ru17	0.26025	0.59736	0.1793
C43	0.22039	0.43146	0.06996	Ru18	0.35072	0.48656	0.20187
C44	0.66408	0.65452	0.04593	Ru19	0.35592	0.3052	0.30789

C45	0.71984	0.76552	0.05203	Ru20	0.43424	0.38066	0.21048
C46	0.66467	0.98677	0.07313	Ru21	0.53135	0.30324	0.1563
C47	0.82955	0.6543	0.06411	Ru22	0.72967	0.39493	0.14874
C48	0.38619	0.93316	0.07438	Ru23	0.36004	0.79242	0.16908
C49	0.88596	0.76534	0.0635	Ru24	0.34703	0.61476	0.2784
C50	0.83045	0.15301	0.07439	Ru25	0.4592	0.69594	0.18948
C51	0.32985	0.15382	0.06369	Ru26	0.25737	0.41136	0.29475
C52	0.83094	0.82099	0.05789	Ru27	0.46207	0.81204	0.26446

Table S12

Table S12 Comprehensive GC×GC TOF-MS measurement conditions

GC		**SSM**		**TOF-MS**	
Column oven	70, 2 min; 2 ℃/min, 300℃, 10 min	Inlet temperature[a]	+0 ℃	Ion source temperature	230 ℃
Carrier gas	He (99.999%)	Outlet temperature[a]	+30 ℃	MS transmission line temperature	280 ℃
Flow rate	1.1 mL·min^{-1}	Cold sector temperature	-51 ℃	Ionization voltage	-70 eV
Injection port	300 ℃	Modulation period	5 s	Mass range	40-1200 amu
Sample volume	1 mL			Scan rate	50 times /s
Split ratio	20:1				

[a] Relative to GC column temperature.

Figure S14

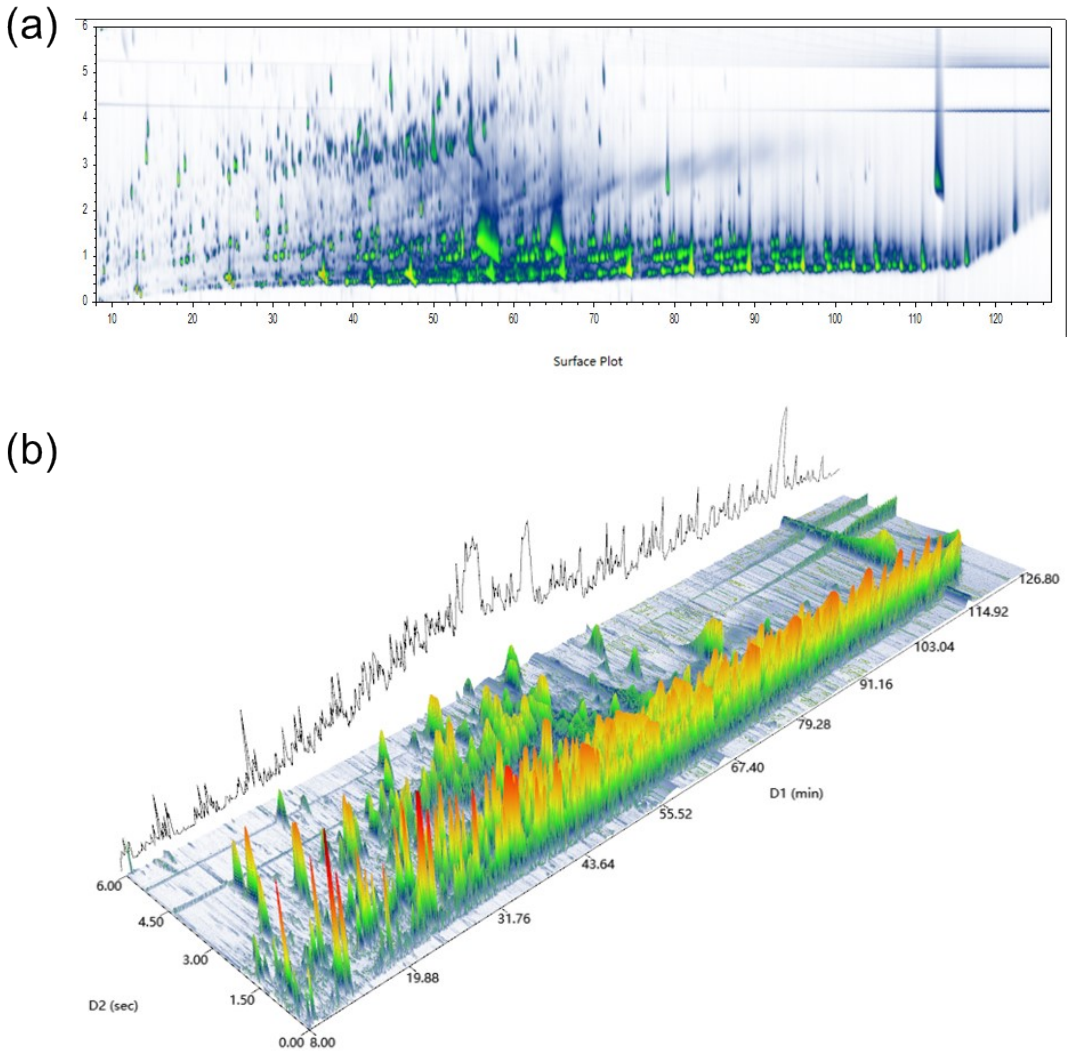

Figure S14. Comprehensive GC×GC TOF-MS spectra of 2d view (a) and 3d view (b) of lignin depolymerization products catalyzed by RuMo/rGO(10-1). Conditions: 1 mg RuMo/rGO(10-1), 10 mg previously prepared organosolv lignin powder, 0.3 MPa O_2, 100℃, 12h, pH=12. Sample was pre-extracted with ethyl acetate and n-hexane before GC×GC TOF-MS measurement. Products were RI calibrated by nC7-nC35 n-alkanes and then identified by the NIST 17 mass spectral library.

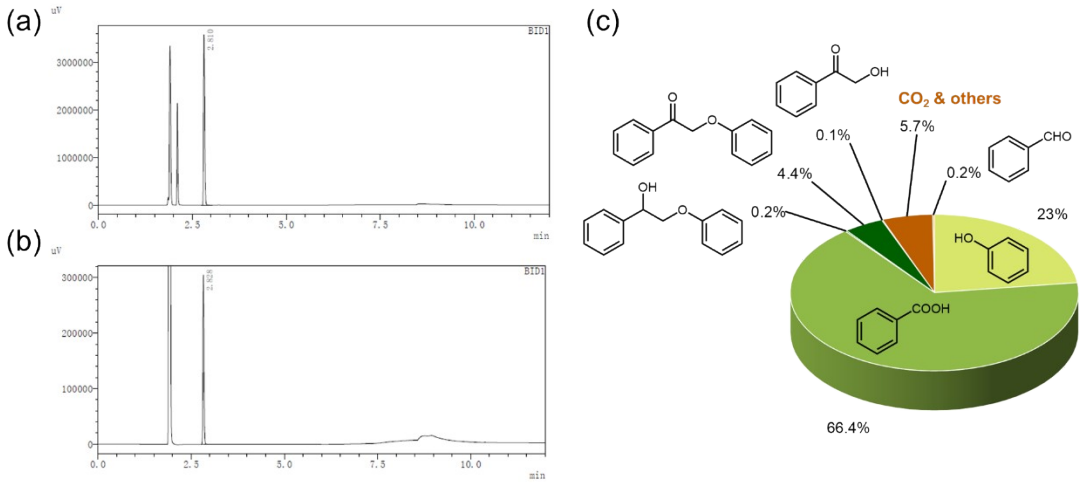

Figure S15. The corresponding GC-MS data of the (a) CO_2 standard sample (CO_2 containing 9.81%, at t_R = 2.8 min) and (b)gaseous atmosphere of the oxidative cleavage reaction of 2-phenoxy-1-phenylethanol using RuMo/rGO(10-1) as catalyst; (c) the as-estimated carbon balance of the reaction. Reaction conditions: 0.2 mg RuMo/rGO(10-1) 0.01 mmol 2-phenoxy-1-phenylethanol, 0.3 MPa O_2, 100 °C, 12 h, pH = 12.

Table S13 Conversion and yield of the 5 times larger scaled reaction of oxidative cleavage of 2-phenoxy-1-phenylethanol

Conversion /%	Yield / %				
	Phenol	Benzoic acid	2-phenoxy- 1-phenylethan-1-one	α-hydroxyacetophenone	others
99	77	75	21	2	<1

Table S14 RuMo/rGO(10-1) catalyst recover mass in each run for the reuseability assessment experiments.

Cycle time(s)	Catalyst mass / mg	Absorbance / a.u.
0	0.2031	0.271
1	0.1863	0.249
2	0.1825	0.244
3	0.1710	0.229
4	0.1626	0.218
5	0.1596	0.214

6	0.1497	0.201

[a]Acquired and calculated from a mass-to-absorbance standard curve from catalysts' absorbance in each run.

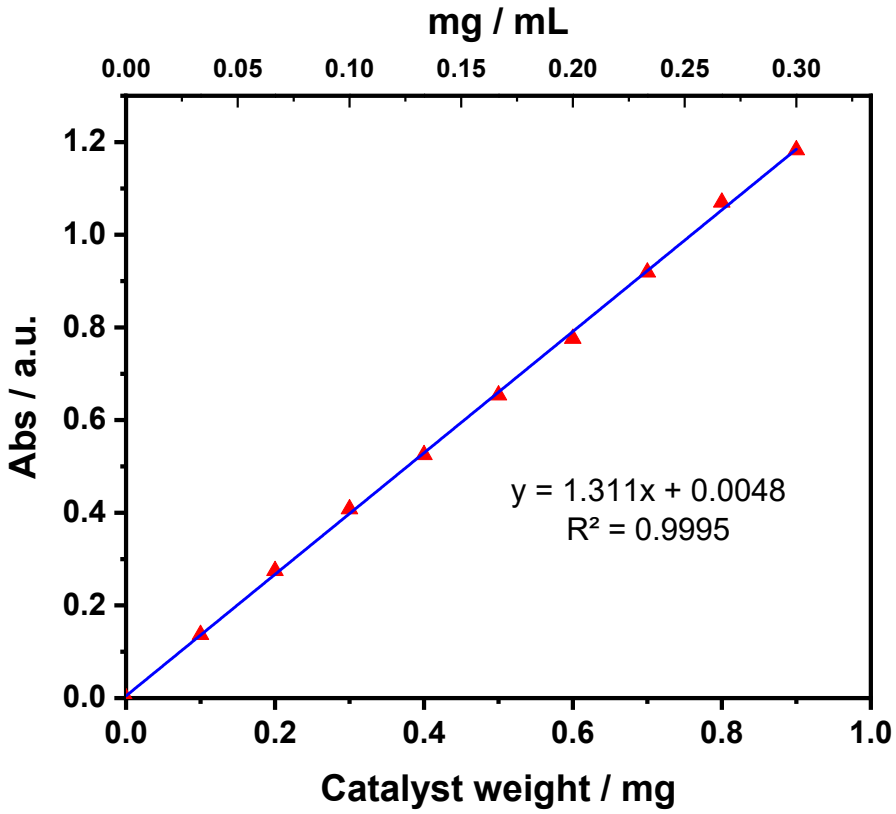

Figure S16. RuMo/rGO(10-1) catalyst weight(mg)-to-absorbance(a.u.) standard curve. Measured at λ = 235 nm in a 3 mL quartz cuvette.

References

1. J. Zhang, H. Yang, G. Shen, P. Cheng, J. Zhang and S. Guo, *Chem. Commun. (Camb)*, 2010, **46**, 1112-1114.
2. J. Zhang, P. Lei, D. Yu, Y. Li, M. Zhong, W. Shen and S. Guo, *Chem.*, 2023, **29**, e202203144.
3. W.-L. Song, Q. Dong, L. Hong, Z.-Q. Tian, L.-N. Tang, W. Hao and H. Zhang, *RSC Adv.*, 2019, **9**, 31070-31077.
4. L. Zhao, S. Shi, G. Zhu, M. Liu, J. Gao and J. Xu, *Green Chem.*, 2019, **21**, 6707-6716.
5. W. Deng, H. Zhang, X. Wu, R. Li, Q. Zhang and Y. Wang, *Green Chem.*, 2015, **17**, 5009-5018.
6. S. Liu, L. Bai, A. P. van Muyden, Z. Huang, X. Cui, Z. Fei, X. Li, X. Hu and P. J. Dyson, *Green Chem.*, 2019, **21**, 1974-1981.
7. J. Liang, M. X. Wang, Y. P. Zhao, W. W. Yan, X. G. Si, G. Yu, J. P. Cao and X. Y. Wei, *ChemCatChem*, 2021, **13**, 3836-3845.
8. G. Kresse and J. Hafner, *Phys. Rev. B*, 1994, **49**, 14251-14269.

9. G. Kresse and J. Hafner, *Phys. Rev. B*, 1993, **47**, 558-561.
10. G. Kresse and J. Furthmüller, *Comp. Mater. Sci.*, 1996, **6**, 15-50.
11. G. Kresse and J. Furthmüller, *Phys. Rev. B*, 1996, **54**, 11169-11186.
12. J. P. Perdew, K. Burke and M. Ernzerhof, *Phys. Rev. Lett.*, 1996, **77**, 3865-3868.
13. G. Kresse and D. Joubert, *Phys. Rev. B*, 1999, **59**, 1758-1775.
14. P. E. Blöchl, *Phys. Rev. B*, 1994, **50**, 17953-17979.